Ultrafast Science
A SCIENCE PARTNER JOURNAL

RESEARCH ARTICLE

All-PM Fiber Mamyshev Oscillator Delivers Hundred-Nanojoule and Multi-Watt Sub-100 fs Pulses

Tao Wang, Can Li*, Bo Ren, Kun Guo, and Pu Zhou*

College of Advanced Interdisciplinary Studies, National University of Defense Technology, Changsha 410073, China.

*Address correspondence to: lc0616@163.com (C.L.); zhoupu203@163.com (P.Z.)

Citation: Wang T, Li C, Ren B, Guo K, Zhou P. All-PM Fiber Mamyshev Oscillator Delivers Hundred-Nanojoule and Multi-Watt Sub-100 fs Pulses. *Ultrafast Sci.* 2023;3:Article 0016. https://doi.org/10.34133/ultrafastscience.0016

Submitted 2 August 2022
Accepted 2 January 2023
Published 8 March 2023

An all-fiber Mamyshev oscillator with a single amplification arm is experimentally demonstrated to achieve high-energy and high-average-power ultrafast pulse output, with the initiating of an external seed pulse. In the high-energy operation, a maximum single-pulse energy of 153 nJ is achieved at a repetition rate of 9.77 MHz. After compression with a pair of diffraction gratings, a measured pulse width of 73 fs with a record energy of 122.1 nJ and a peak power of 1.7 MW is obtained. In the high-average-power operation, up to 5th harmonic mode locking of the oscillator is realized via slightly adjusting the output coupling ratio and the cavity length. The achieved maximum output power is 3.4 W at a repetition rate of 44.08 MHz, while the corresponding pulse width is compressed to around ~100 fs. Meanwhile, the system is verified to be operated reliability in both high-energy and -average-power operation regimes through assessing its short- and long-term stabilities. To the best of our knowledge, these are the highest records in pulse energy and average power delivered from a single all-fiber ultrafast laser oscillator with picosecond/femtosecond pulse duration. It is believed that even higher-energy and -average-power ultrafast laser can be realized with the proposed laser scheme through further increasing the core diameter of the all-fiber cavity, providing promising sources for advanced fabrication, biomedical imaging, laser micromachining, and other practical applications, as well as an unprecedented platform for exploring undiscovered nonlinear dynamics.

Introduction

Ultrafast lasers emitting picosecond/femtosecond pulses have been extensively researched over decades [1–5], thanks to the aplenty of operation regimes and nonlinear phenomena that are unveiled and yet to be explored. In addition, compared with their solid-state counterparts, fiber lasers have intrinsic advantages such as compact and robust structure, high efficiency, excellent anti-interference ability, and high beam quality [6–8]. Nevertheless, an indispensable precondition for keeping all those merits is the implementing of an all-fiber laser configuration, which, however, would hinder the scaling of the average power and pulse energy, owing to the strong nonlinearity that induced by the interaction of intense light confined in the small mode area and the long fiber waveguide, rendering it unable to compete with solid-state lasers in terms of output power and energy under ultrafast operation [9]. To a certain degree, this issue can be circumvented by exploiting the fiber chirped pulse amplification scheme with large mode area (LMA) fiber and cladding pumping, and impressive results such as 300-W average power [10] and 150-μJ single-pulse energy [11] have been achieved with an all-fiber format. However, higher output power and energy from a single fiber oscillator are still desirable for simplifying or even removing the subsequent amplification stages for specific applications and provide an unprecedented platform for exploring undiscovered nonlinear dynamics.

The convention method to obtain high-energy pulse output is the implement of an all-normal dispersion fiber laser, in which the intracavity pulse is highly chirped such that the accumulated nonlinear phase can be alleviated with a broadened duration and reduced peak power. Typical operation mechanisms are the dissipative soliton and similariton mode locking, which are well-known nonlinear attractors of all-normal dispersion mode-locked fiber lasers and can generally emit nanojoule-level pulse energy [12–16]. Enlarging the core diameter of the fiber and extending the cavity length are two ways to further increase the pulse energy, and in this case, the light intensity is reduced in the space domain, as well as extending the cavity length, to augment the time chirping and reduce the pulse repetition rate. In 2015, a dissipative soliton mode-locked fiber laser constructed with LMA 10/125 fiber was demonstrated to emit over 50-nJ single-pulse energy at a repetition rate of 1.44 MHz (cavity length, 138 m), which corresponds to an average power of ~70 mW [17]. Subsequently, a similar work with an output pulse energy of 50 nJ and a repetition rate of 5.3 MHz (cavity length, 40 m) was reported in [18] using the same fiber, and further pulse enhancement is limited by strong Raman effect. Considering the average power scaling, there is actually a dilemma with the cavity length of mode-locked fiber lasers. As a short cavity length can lead to a high repetition rate of the yielded pulse train and then an increased output power, the overall optical gain inside the cavity would be limited with the decreased length of the

gain fiber. In this way, the output power of ultrafast all-fiber laser is generally in the tens of milliwatt level, and, up to now, the maximum is 308 mW with a repetition rate of 71 MHz [19]. Basically, there is no substantial scheme to simultaneously achieving high pulse energy and average power from a single ultrafast all-fiber laser. Although the dissipative soliton resonance mode locking can realize watt-level power pulsing with hundreds of nanojoule energy [20,21], its pulse width is nanosecond level with nonlinear chirping and can hardly be compressed to the ultrafast regime.

Recently, the mode-locked fiber Mamyshev oscillator (MO) has attracted much attention because of its potential to produce high-power and high-energy pulses with ultrashort duration [22–37]. Essentially, the mode-locking mechanism of MO is based on the nonlinear spectral broadening and offset spectrum filtering at 2 cascaded fiber amplification arms [22]. In this way, energetic pulsing could be realized through delicately engineer the cavity design, while the continuous light and weak pulses will be blocked by the filtering. Up to now, the maximum pulse energy of 1 μJ and the average power of 9 W have been achieved from an MO based on LMA photonic crystal fiber, which, however, incorporates free-space coupling to form the cavity, rendering the system cumbersome and susceptible to interference [25].In 2020, the first all-fiber MO was reported in [34], and >20-nJ pulse energy at fundamental repetition rate and 1.3-W average power at 14th harmonics (107.8 MHz) are obtained, whereas the outputted pulse was not compressed. In 2021, an all-fiber harmonic mode-locked MO that operates at 305-MHz repetition rate was demonstrated; however, the pulse energy was just few nanojoules owing to the using of 6/125 fiber [35]. After that, we demonstrated an all-10/125-fiber MO and achieved the maximum pulse energy of 83.5 nJ with the output power of 787.3 mW [36]. More recently, an all-fiber MO with the association of active and passive arm that mode-locked at the fundamental repetition rate was realized with 110-nJ pulse energy, which was reduced to 80 nJ after compression, and the limitation for further energy scaling might be attributed to the inclusion of small-mode-area fiber in the cavity [37].

Here, we experimentally demonstrate an ultrafast laser that leveraging a polarization-maintaining (PM) all-10/125-fiber MO with a single amplification arm, while the other arm is replaced with a segment of transmission fiber. With such a simplified structure, the achieved maximum single-pulse energy is 153 nJ with an average power of 1.5 W at a repetition rate of 9.77 MHz. The pulse width could be externally compressed to 73 fs by a pair of diffraction gratings. Considering the insertion loss of the gratings, the compressed pulse has the maximum single-pulse energy of 122.1 nJ with a maximum peak power of 1.7 MW, standing for a new milestone of the all-fiber ultrafast lasers, which has never realized hundred-nanojoule energy before. Through adjusting the output coupling ratio, we obtained the maximum output power of 3.4 W at the 5th harmonic repetition rate (44.08 MHz), corresponding to a pulse energy of 77.1 nJ. Moreover, the pulse width can be compressed to around ~100 fs at the maximum power. These results are verified to show good stability against environmental interference and can operate stably for several h. To the best of our knowledge, both 153-nJ pulse energy and 3.4-W average power are the highest record from all-fiber-based picosecond or femtosecond ultrafast laser oscillators. This progress is one important step closer toward achieving both hundred-nanojoule energy and ten-watt power from a compact all-fiber ultrafast laser cavity.

Materials and Methods

The experimental setup for the hundred-nanojoule level all-fiber MO is shown in Fig. 1. Different from a common MO, the current structure comprises only one amplification arm with 2 offset filters, of which the central wavelength/3-dB bandwidth

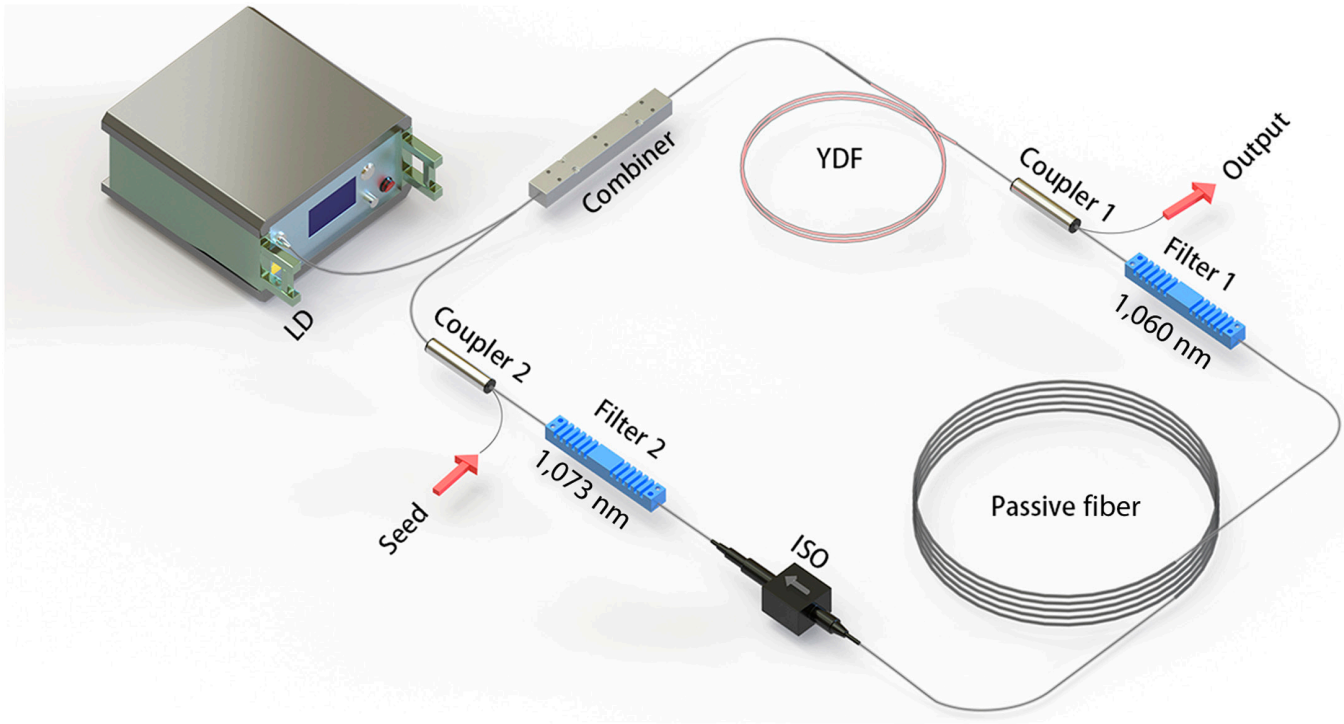

Fig. 1. Experimental setup for the hundred-nanojoule level all-fiber MO. LD, laser diode; ISO, isolator.

is respectively 1,060 nm/10 nm (filter 1) and 1,073 nm/7 nm (filter 2). The active gain fiber is a piece of 2.6-m 10/125 Yb-doped fiber (YDF) with the absorption coefficient of 4.95 dB/m at 976 nm and is forward pumped by a multimode laser diode via a combiner. The coupler 1 is connected after the YDF to export 80% of laser energy out the cavity. A segment of 10-m passive fiber is inserted between the 2 filters for spectrum broadening, along with an optical isolator to guarantee unidirectional circulation of the laser in the cavity. In addition, the coupler 2 with a coupling ratio of 40:60 is placed before the amplification arm to introduce a pulse seed into the cavity for initiating the mode-locking operation. The total cavity length is about ~ 21.2 m, corresponding to the fundamental repetition rate of 9.77 MHz. It should be noted that the cavity is an all-PM structure, in which all pig tails of the optical components are PM 10/125 fiber. Such a new variation of MO with only one gain arm makes the system more compact, integrated, and convenient to be manipulated without the need to regulate the power of 2 pump laser diodes. To characterize the laser pulse, an optical power meter, and an optical spectrum analyzer with a resolution of 0.02 nm, a photodetector with a bandwidth of 5 GHz, an oscilloscope with a bandwidth of 1 GHz, a radio frequency (RF) analyzer with a resolution of 1 Hz, and an autocorrelator were employed to monitor the output port of coupler 1. The pulse seed that initiates stable pulsing of the MO was a home-made mode-locked laser with a repetition rate of 19.82 MHz and a pulse width of 10 ps. As the output laser pulse will be highly chirped, a diffraction grating pair with a line density of 1,000 lines/mm was utilized to construct a folded Treacy grating compressor to dechirp it to the femtosecond regime.

Results and Discussion

High-energy operation

With the gradual increase in the pump power, a transition of the output from amplified seed pulse to multipulse and then stable mode-locked pulse with the fundamental repetition rate of the cavity was observed on the oscilloscope. Once stable mode locking is established, it can be maintained with the ceasing of the seed pulse. In the current experiment, the mode locking of the MO could be operated stably for a pump power range from 3.4 to 5.6 W. Figure 2A shows the evolution of the output power with the enhancement of pump power, manifesting a linear relationship with a slope efficiency of 68.2%. Under the pump power of 5.6 W, a maximum output power of 1.5 W was obtained, corresponding to a maximum single-pulse energy of 153.0 nJ. With the increase in the output pulse energy, a gradual broadening of the optical spectrum was observed because of the intensified nonlinearity, as shown in Fig. 2B. Meanwhile, remarkable stimulated Raman scattering (SRS) component also

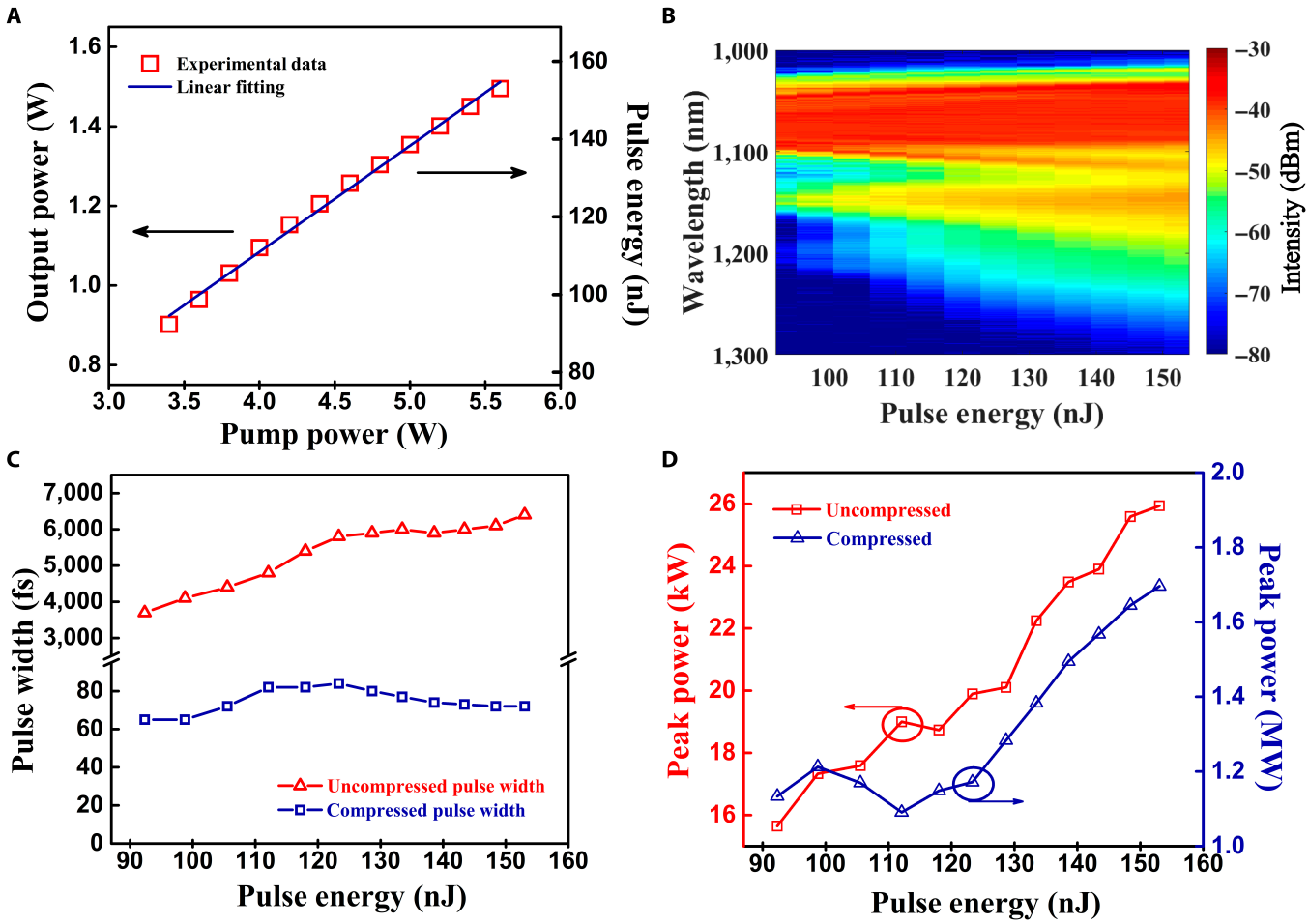

Fig. 2. Pulse characteristics of the high-energy MO. (A) Output power and single-pulse energy versus the pump power. (B) Evolution of the output optical spectrum, (C) the measured pulse width before and after compression, and (D) the corresponding calculated peak power with the increase in the single-pulse energy.

emerged with the increase in the pulse peak power. The measured duration and peak power of the output pulse before and after dechirping are respectively shown in Fig. 2C and D. Because of the broadened spectrum at higher energy, the uncompressed pulse width demonstrates a monotonous widening from 3.7 to 6.4 ps, whereas after compression, the pulse width stays around 75 ± 10 fs, indicating that the accumulated pulse chirping at higher energy can basically be compensated with the grating compressor. In addition, the calculated pulse peak power demonstrates a similar trend versus the increase in the energy before and after compression, with the maximum value of 25.9 kW and 1.7 MW, respectively (considering the 1.05-dB insertion loss of the compressor). It is also noted that the peak power achieved from this single all-fiber oscillator is in the same order of magnitude as that obtained from an all-fiber chirped pulse amplifier [38,39]. The optical spectrum at the maximum power of 1.5 W is presented in Fig. 3A, in which the 10-dB bandwidth is around 60 nm. It is observed that the long wavelength SRS light is 7 dB lower than the signal light, and through integral calculation of the spectrum from 1,100 to 1,300 nm, its weight is about 18.7% in the total output power. Moreover, despite the prominent SRS effect compared with conventional mode-locked lasers, it is inferred to be originated from weak signal that shifted to the long wavelength via self-phase modulation other than random noise, as the overall performance of the laser pulse is commendable as will be discussed later. In addition, it is noted that the spectral spikes at around 1,030 nm are attributed to the combined effects of nonlinear and linear gain, with the latter being particularly high for the YDFs, as, at this spectral range, the continuous wave components are unlikely to survive considering the passbands (1,060 and 1,073 nm) of the intracavity filters. The measured autocorrelation trace of the compressed pulse at maximum energy is shown in Fig. 3B, demonstrating a 3-dB pulse width of 73 fs, while the slight pedestal should be attributed to the uncompensated nonlinear chirping that induced by high-order dispersion and nonlinear effects including SRS, which is prominent on the measured output spectrum as shown in Fig. 3A. The inset presents the corresponding autocorrelation trace in a temporal span of 15 ps, in which no satellite pulses are observed.

The pulse characteristics were further examined at the pump power of 5 W (138.6-nJ pulse energy) to verify the system reliability and stability. Figure 4A shows the measured pulse train (top part), of which the pulse interval is 102.4 ns, corresponding to the fundamental repetition rate of 9.77 MHz. The bottom part of Fig. 4A shows the pulse envelope of a single pulse detected by a high-speed photodetector with bandwidth of 12.5 GHz and a real-time oscilloscope with a bandwidth of 36 GHz, indicating the single-pulse operation of the MO. Besides, the amplitudes of output pulses are counted and normalized relative to the maximum. Figure 4B presents the amplitude histogram of 10,000 pulses that are normalized to the maximum, manifesting a normal distribution of the pulse intensity within a narrow range. In addition, the ratio of the standard deviation of pulse amplitudes to the mean value is calculated to be 1.8%. The RF spectrum is depicted in Fig. 4C with a span of 40 kHz and a resolution of 1 Hz and illustrates a signal-to-noise ratio as high as 81.2 dB (over 130,000,000 contrast). Figure 4D demonstrates the intensity profile of the output laser beam after collimation with a lens, indicating a strict single-mode operation of the high-energy MO.

The long term stability of the high-energy MO system was evaluated by monitoring the output power and optical spectrum simultaneously through leveraging a 1‰ coupler for 5 h. The average power recorded per second is shown in Fig. 5A, where the calculated root mean square fluctuation is less than 0.26%. The optical spectrum evolution was examined every 20 s during the monitoring process, and the results is shown in Fig. 5B, in which no significant variation is observed.

High-average-power operation

On the basis of the high-energy operation, a straightforward strategy to obtain high-average-power output is to make the oscillator operating in the harmonic mode-locking regime, which, in the current work, is realized through modifying the coupling ratio of coupler 1 in Fig. 1 from 20:80 to 30:70. In addition, the total cavity length was slightly increased to ~23.5 m, corresponding to the fundamental repetition rate of 8.82 MHz.

During the experiment, up to 5th harmonic mode locking was realized with the increase in the pump power with a fixed

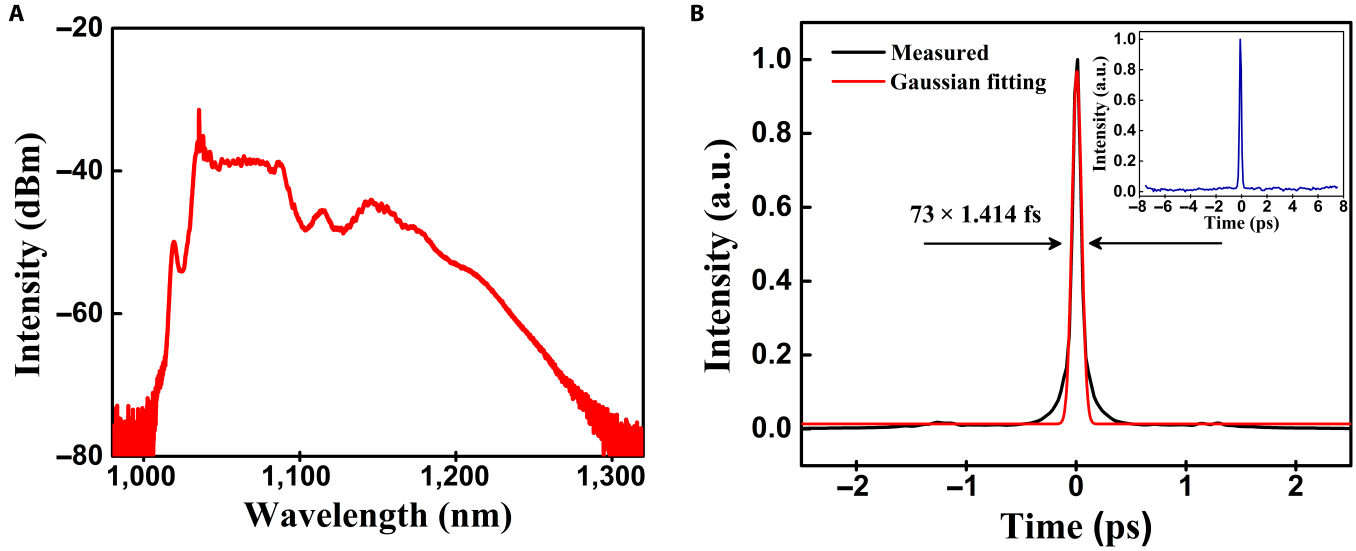

Fig. 3. Pulse characteristics at the maximum output power. (A) Optical spectrum and (B) autocorrelation trace of the compressed pulse. Inset: Autocorrelation trace recorded in a temporal span of 15 ps. a.u., arbitrary units.

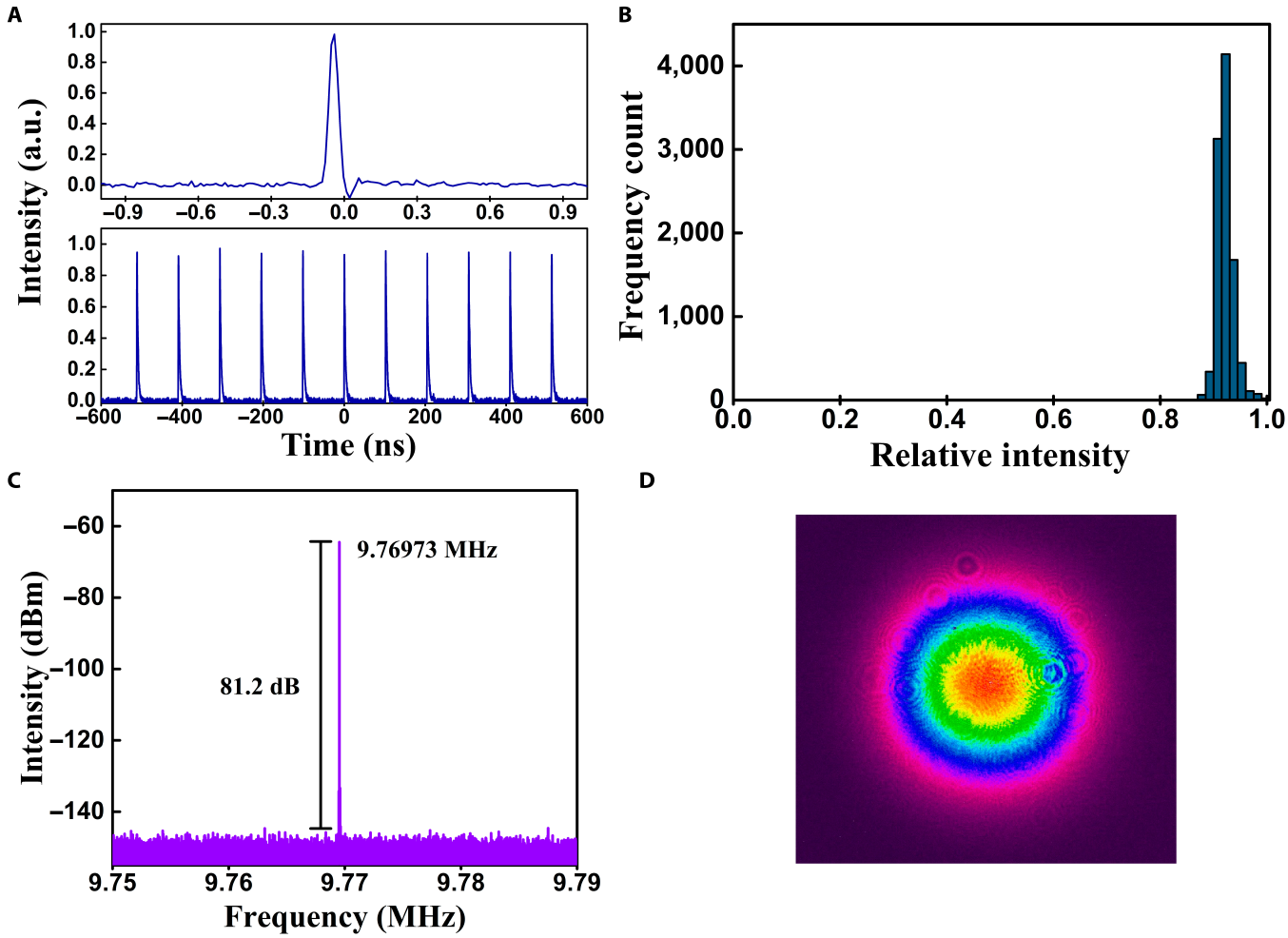

Fig. 4. Pulse properties at the pump power of 5 W. (A) Top: Pulse train. Bottom: Envelope of a single pulse. (B) The statistical amplitude histogram of 10,000 pulses that are normalized to the maximum. (C) RF spectrum of the fundamental frequency. (D) Beam profile of the output laser pulse after collimation.

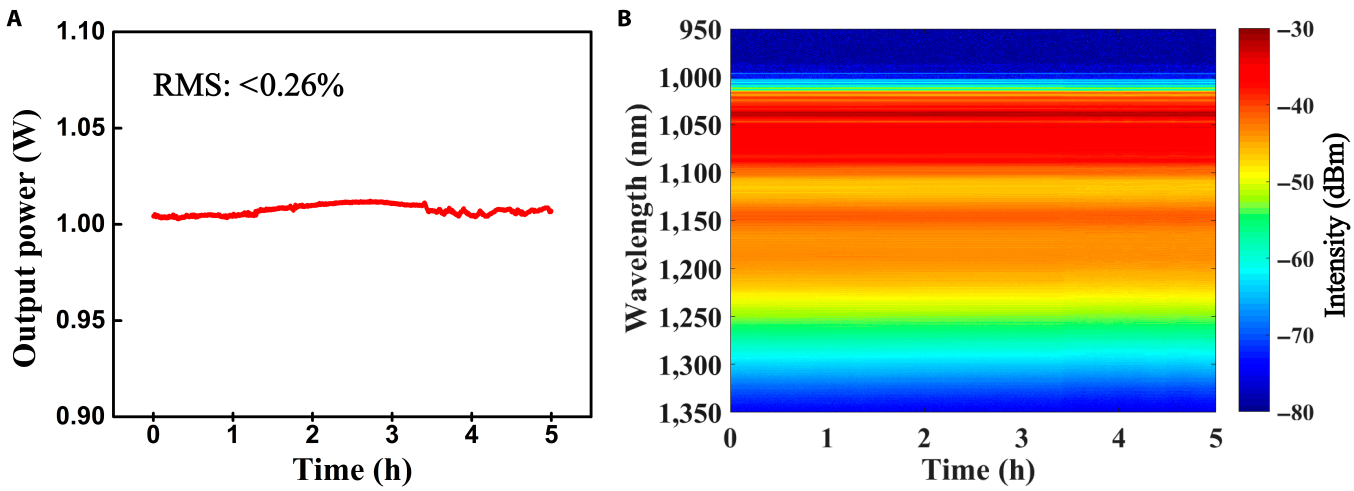

Fig. 5. Long-time stability of the high-energy MO within 5 h. (A) Output power recorded every second. (B) Optical spectrum evolution recorded every 20 s.

injecting seed power, which can be turned off once stable pulsing operation was established. Figure 6A demonstrates the 1st, 2nd, 3rd, 4th, and 5th harmonic pulse trains with the repetition rates of 8.82, 17.63, 26.45, 35.26, and 44.08 MHz, respectively, showing periodic pulses without satellite peaks. The corresponding spectra at the highest power of each order of harmonics are shown in Fig. 6B, which manifests similar profiles that comprise the main signal and the SRS components, probably owing to the commensurate maximum peak powers inside the cavity. The maximum power and corresponding energy with the increase

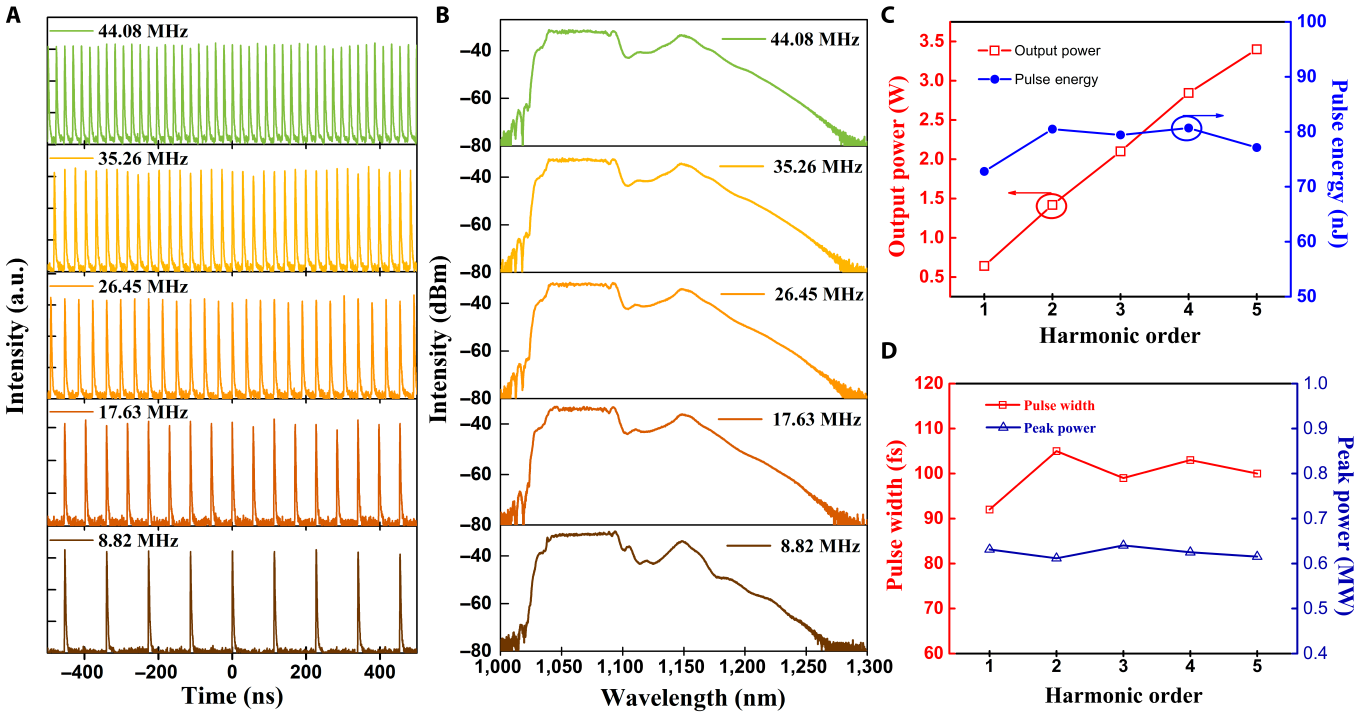

Fig. 6. Pulse characteristics of the harmonic mode-locked MO. (A) Pulse trains and (B) spectra at different operation repetition rates. (C) The maximum output power/single-pulse energy and (D) dechirped pulse width/peak power as a function of harmonic order.

in the harmonic order are depicted in Fig. 6C, in which the power enhancement presents a quasi-linear manner, echoing with the increase in the pump power. The maximum power of 3.4 W is achieved at the 5th harmonic, beyond which the system would turn into multipulse operation. In addition, the highest single-pulse energy at each harmonic is around 80 nJ, owing to the peak power clamping effect inside the cavity. Comparing with the high-energy operation, the relatively lower achievable maximum energy in the current operation regime is attributed to the higher power circulating in the cavity. Figure 6D presents the compressed pulse width and peak power at the highest power of each order of harmonics. Similar to the single-pulse energy, the dechirped pulse width is around 100 fs, while the corresponding calculated peak power is around 0.63 MW after taking into account the insertion loss of the compressor.

The pulse characteristics were further examined in detail at the 5th harmonic mode locking. The output power evolution with a linear slope efficiency of 69.4% versus pump power increasing from 6.1 to 11 W is shown in Fig. 7A, which also demonstrates the single-pulse energy increasing from 43.3 to 77.1 nJ. Figure 7B shows the pulse width before and after compression as a function of output power. It is observed that before compression, the pulse width is gradually increased from 1 ps to around 2.5 ps, associating with the broadening of the optical spectrum. After compression, the pulse width stays around 90 fs, and the minimum duration is measured to be 83 fs at the output power of 2.68 W. The optical spectrum evolution with the enhancement of the operation power is shown in Fig. 7C, in which a similar spectral broadening effect with the high-energy operation version can be observed. The autocorrelation profile of the compressed pulse at the maximum power is shown in Fig. 7D, and the Gaussian fitting indicates a pulse width of 100 fs. The small side peaks observed in the Fig. 7D are attributed to the more excessive nonlinearity and uncompensated high-order dispersion. As in the harmonic mode locking (HML) regime, the pulse width was narrowed by more than 2.5 times, the corresponding peak power and, thus, the nonlinear effect were significantly increased accordingly.

The system stability and reliability were also assessed at the pump power of 10 W, corresponding to an output power of 3.11 W. Figure 8A demonstrates the measured RF spectrum with a peak frequency of 44.08 MHz and a signal-to-noise ratio of ~73 dB. To examine the supermode noise of the harmonic mode-locking operation, the RF spectra were measured in a frequency range of 50 MHz at the highest output power of each order of harmonic. It was observed that the supermode noise gradually emerges with the increase in the order of harmonic and, at the maximum output power of 3.4 W, the suppression of the base mode to the adjacent modes is more than 44 dB (shown in the inset of Fig. 8A), which is comparable to that in previous reported harmonic mode-locked MO with much lower pulse energy [34]. In addition, the histogram distribution of the amplitude of 10,000 pulses is presented in Fig. 8B, showing a similar behavior with that of the high-energy operation version. The calculated ratio of the standard deviation of the recorded pulse amplitudes to its mean value is 1.7%. The inset in Fig. 8B depicts the intensity profile of the output beam after collimation, and the strict single-mode characteristic of the high-average-power working is verified. The power and optical spectrum evolution within 5 h are respectively demonstrated in Fig. 8C and D, showing stable output power with root mean square variation of less than 0.12% and spectral constancy.

It should be pointed out that Bednyakova et al. [40] theoretically and experimentally analyzed the dynamics of a harmonics mode-locked MO, which is explained by the dissipative Faraday instability (DFI) mechanism. The DFI is based on the fact that a pattern in the temporal domain will be produced by

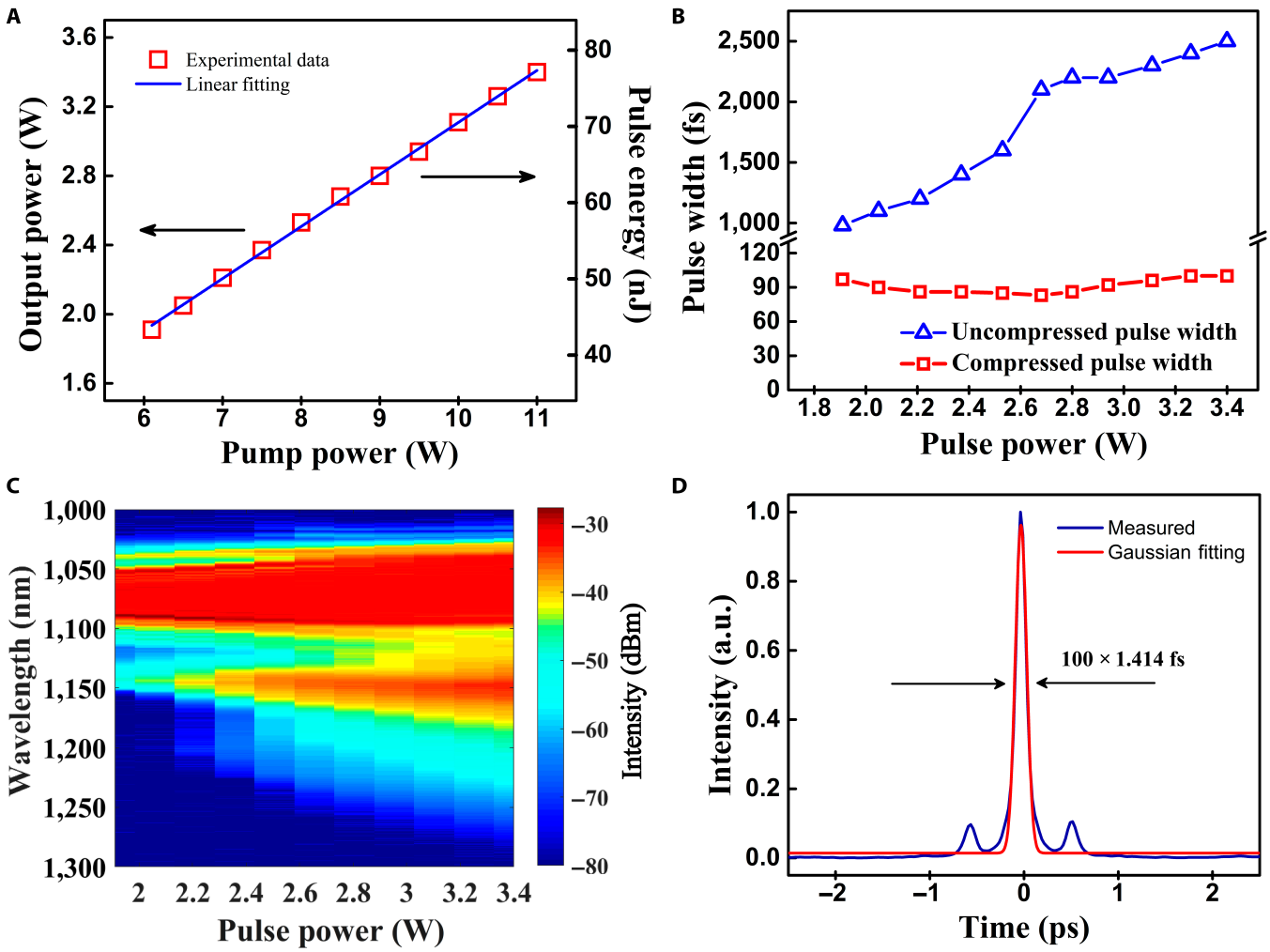

Fig. 7. Pulse characteristics under the 5th harmonic mode-locking operation. (A) Output power and single-pulse energy versus the pump power. (B) The variation of pulse width before and after compression and (C) spectra with the increase in output power. (D) The autocorrelation profile of the compressed pulse at the maximum output power.

alternating spectral dissipative windows, which triggers harmonic mode-locking or multipulse operation [41]. In [40], 2 wavelength-adjustable filters were introduced, for inducing multipulse or harmonic mode-locking operation by changing the separation of the 2 filters. However, in our work, the HML was obtained with the increase in the pump power, while the filters are unadjustable. Besides, during the start-up of the HML, the pulses were observed to be first randomly distributed and then redistributed evenly, indicating a manner disagrees with the DFI model while agrees with the theory of gain depletion and recovery [35,42] , which is recognized as the general process of conventional HML fiber lasers and has been verified to be applicable to HML operation in MO [35]. Considering the triggering of HML in our work, it may be inappropriate to simply attribute to the reinforced nonlinearities in the cavity. According to the theory of gain depletion and recovery, an increased portion of the pulse energy circulating inside the cavity would strengthen the depletion of the gain and then facilitate the acceleration of pulses and the formation of harmonic mode locking. This can be verified by the narrowed pulse width (maximum of 2.5 ps) compared with that operated in the high-energy regime (maximum of 6.4 ps). In addition, as the cavity length is also increased by ~2 m, the fundamental repetition rate is accordingly reduced, and the intracavity nonlinearities would be increased to some degree, further assisting the onset of HML operation.

Conclusion

In conclusion, an all-fiber PM MO system that delivers hundred-nanojoule energy and multiwatt power ultrafast laser was experimentally demonstrated with a single amplification arm inside the cavity and an external seed pulse. In the high-energy operation, the maximum single-pulse energy of 153 nJ was achieved at the repetition rate of 9.77 MHz, corresponding to 1.5-W average power. The pulse width was externally compressed to 73 fs with 122.1-nJ pulse energy by a pair of diffraction gratings, resulting a maximum peak power of 1.7 MW. In the high-average-power operation, up to 5th harmonic mode locking of the all-fiber MO was realized with the repetition rate of 44.08 MHz, through slightly modifying the output coupling ratio and the cavity length. The maximum output power was 3.4 W with a single-pulse energy of 77.1 nJ, and the dechirped pulse width was around ~100 fs. The reliability and short-/long-term stability of both operation regimes were verified through characterizing its temporal, frequency, and space

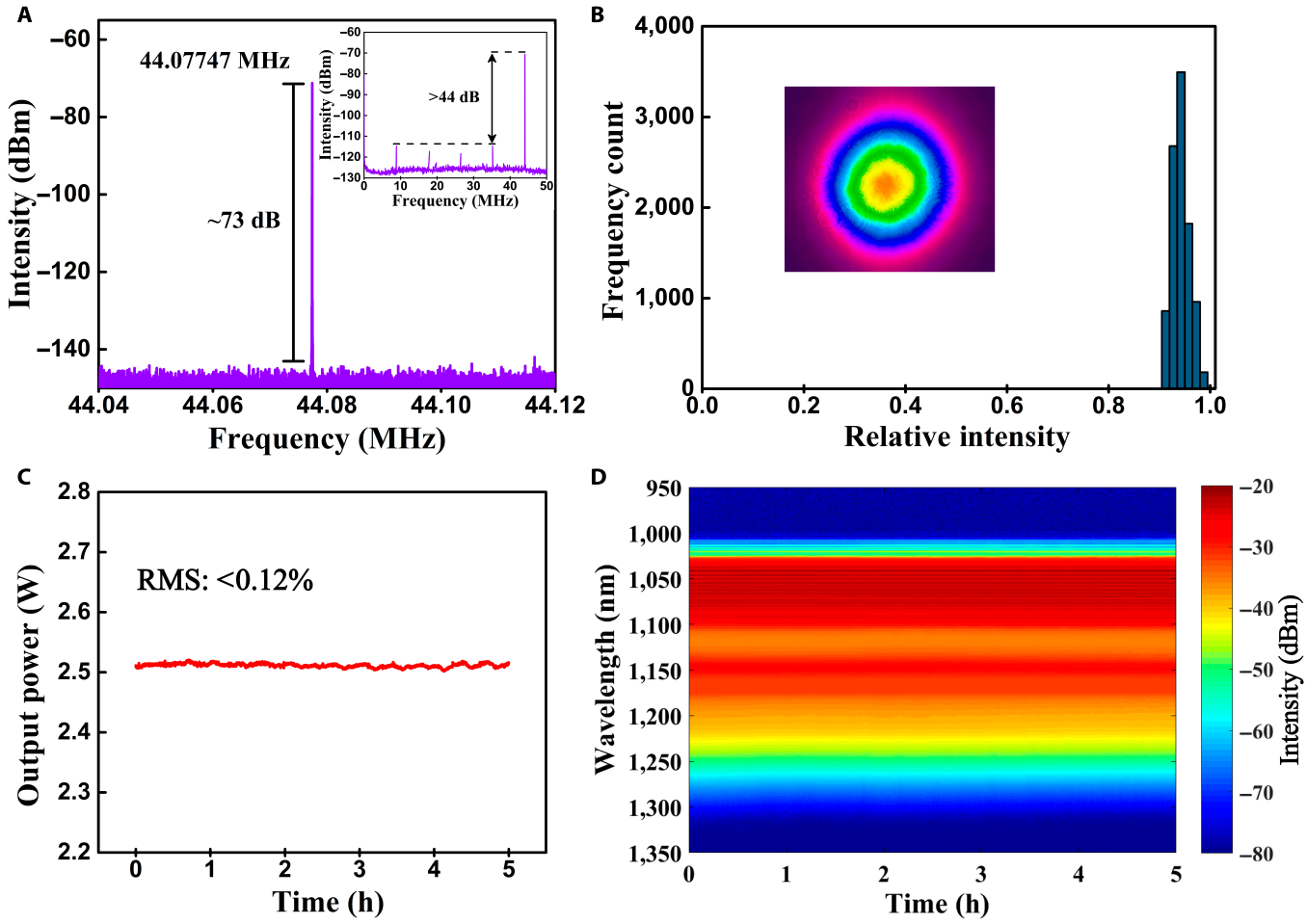

Fig. 8. Pulse stability properties at pump power of 10 W. (A) RF spectrum at the base frequency of the 5th harmonics. Inset: The RF spectrum in a wider spectrum range of 0 to 50 MHz. (B) The statistical histogram of the amplitude of 10,000 pulses relative to its maximum. Inset: The intensity profile of the output laser beam after collimation. (C) The output power (recorded every second) and (D) optical spectrum evolution (recorded every 20 s) within 5 h.

domain properties. To the best of our knowledge, this is the highest pulse energy and average power emitted from an all-fiber ultrafast laser oscillator with picosecond/femtosecond pulse duration. Although, in the current work, the self-started mode locking was not demonstrated mostly because of the fixed central wavelength of the filters, it is expected that through employing wavelength tunable filters, the self-starting operation is readily realizable with routinely method [32,33,37]. Moreover, higher-energy and -power ultrafast laser can be envisioned to be generated with a similar manner through implementing an all-fiber MO with higher core diameter of the fiber and exploiting new nonlinear pulse evolution [43] that has a higher tolerance to the nonlinear phase accumulation.

Acknowledgments

Funding: This work was supported by the National Natural Science Foundation of China under grant 62005316 and Director Fund of State Key Laboratory of Pulsed Power Laser Technology under grant SKL2020ZR02. **Author contributions:** C.L. and P.Z. conceived the idea and designed the experiments. T.W., B.R., and K.G. conducted the experiments. T.W. performed the initial manuscript. C.L. and P.Z. revised the manuscript. **Competing interests:** The authors declare that they have no competing interests.

Data Availability

The data that support the plots within this paper and other findings of this study are available from the corresponding authors upon reasonable request.

References

1. Fermann ME, Hartl I. Ultrafast fibre lasers. *Nat Photonics*. 2013;7:868–874.
2. Malinauskas M, Žukauskas A, Hasegawa S, Hayasaki Y, Mizeikis V, Buividas R, Juodkazis S. Ultrafast laser processing of materials: From science to industry. *Light Sci Appl*. 2016;5(8):e16133.
3. Wise FW, Chong A, Renninger WH. High-energy femtosecond fiber lasers based on pulse propagation at normal dispersion. *Laser Photonics Rev*. 2008;2(1-2):58–73.
4. Zhang J, Pötzlberger M, Wang Q, Brons J, Seidel M, Bauer D, Sutter D, Pervak V, Apolonski A, Mak KF, et al. Distributed Kerr lens mode-locked Yb:YAG thin-disk oscillator. *Ultrafast Sci*. 2022;2022:9837892.
5. Wang X, Liu X, Lu X, Chen J, Long Y, Li W, Chen H, Chen X, Bai P, Li Y, et al. 13.4 fs, 0.1 Hz OPCPA front end for the 100 PW-class laser facility. *Ultrafast Sci*. 2022;2022:9894358.

6. Chang G, Wei Z. Ultrafast fiber lasers: An expanding versatile toolbox. *iScience*. 2020;23(5):101101.
7. Zervas MN, Codemard CA. High power fiber lasers: A review. *IEEE J Sel Top Quantum Electron*. 2014;20(5):219–241.
8. Shi W, Fang Q, Zhu X, Norwood RA, Peyghambarian N. Fiber lasers and their applications [Invited]. *Appl Opt*. 2014;53(28):6554–6568.
9. Fu W, Wright LG, Sidorenko P, Backus S, Wise FW. Several new directions for ultrafast fiber lasers [Invited]. *Opt Express*. 2018;26(8):9432–9463.
10. Yu H, Wang X, Zhang H, Su R, Zhou P, Chen J. Linearly-polarized fiber-integrated nonlinear CPA system for high-average-power femtosecond pulses generation at 1.06 μm. *J Lightwave Technol*. 2016;34(18):4271–4277.
11. Yusim A, Samartsev I, Shkurikhin O, Myasnikov D, Bordenyuk A, Platonov N, Kancharla V, Gapontsev V. New generation of high average power industry grade ultrafast ytterbium fiber lasers. Paper presented at: SPIE Proceedings Vol. 9728 Fiber Lasers XIII: Technology, Systems, and Applications; 11 March 2016.
12. Szczepanek J, Kardaś TM, Michalska M, Radzewicz C, Stepanenko Y. Simple all-PM-fiber laser mode-locked with a nonlinear loop mirror. *Opt Lett*. 2015;40(15):3500–3503.
13. Zhao LM, Bartnik AC, Tai QQ, Wise FW. Generation of 8 nJ pulses from a dissipative-soliton fiber laser with a nonlinear optical loop mirror. *Opt Lett*. 2013;38(11):1942–1944.
14. Erkintalo M, Aguergaray C, Runge A, Broderick NGR. Environmentally stable all-PM all-fiber giant chirp oscillator. *Opt Express*. 2012;20(20):22669–22674.
15. Borodkin A, Honzátko P. High-energy all-PM Yb-doped fiber laser with a nonlinear optical loop mirror. *Opt Laser Technol*. 2021;143:107353.
16. Deng D, Zhang H, Gong Q, He L, Li D, Gong M. Energy scalability of the dissipative soliton in an all-normal-dispersion fiber laser with nonlinear amplifying loop mirror. *Opt Laser Technol*. 2020;125:106010.
17. Zhou J, Gu X, 50.5 nJ, 750 fs all-fiber all polarization-maintaining fiber laser. Paper presented at: Proceedings of the 2015 Conference on Lasers and Electro-Optics (CLEO); 2015 May 10–15; San Jose, CA, California.
18. Kharenko DS, Gonta VA, Babin SA. 50 nJ 250 fs all-fibre Raman-free dissipative soliton oscillator. *Laser Phys Lett*. 2016;13(2):025107.
19. Mortag D, Wandt D, Morgner U, Kracht D, Neumann J. Sub-80-fs pulses from an all-fiber-integrated dissipative-soliton laser at 1 μm. *Opt Express*. 2011;19(2):546–551.
20. Huang Y, Luo Z, Xiong F, Li Y, Zhong M, Cai Z, Xu H, Fu H. Direct generation of 2 W average-power and 232 nJ picosecond pulses from an ultra-simple Yb-doped double-clad fiber laser. *Opt Lett* 2015;40(6):1097–1100.
21. Du T, Luo Z, Yang R, Huang Y, Ruan Q, Cai Z, Xu H. 1.2-W average-power, 700-W peak-power, 100-ps dissipative soliton resonance in a compact Er:Yb co-doped double-clad fiber laser. *Opt Lett*. 2017;42(3):462–465.
22. Regelskis K, Želudevičius J, Viskontas K, Račiukaitis G. Ytterbium-doped fiber ultrashort pulse generator based on self-phase modulation and alternating spectral filtering. *Opt Lett*. 2015;40(22):5255–5258.
23. Liu Z, Ziegler ZM, Wright LG, Wise FW. Megawatt peak power from a Mamyshev oscillator. *Optica*. 2017;4(6):649–654.
24. Sidorenko P, Fu W, Wright LG, Olivier M, Wise FW. Self-seeded, multi-megawatt, Mamyshev oscillator. *Opt Lett*. 2018;43(11):2672–2675.
25. Liu W, Liao R, Zhao J, Cui J, Song Y, Wang C, Hu M. Femtosecond Mamyshev oscillator with 10-MW-level peak power. *Optica*. 2019;6(2):194–197.
26. Olivier M, Boulanger V, Guilbert-Savary F, Sidorenko P, Wise FW, Piché M. Femtosecond fiber Mamyshev oscillator at 1550nm. *Opt Lett*. 2019;44(4):851–854.
27. Boulanger V, Olivier M, Guilbert-Savary F, Trépanier F, Bernier M, Piché M. All-fiber Mamyshev oscillator enabled by chirped fiber Bragg gratings. *Opt Lett*. 2020;45(12):3317–3320.
28. Luo X, Tuan TH, Saini TS, Nguyen HPT, Suzuki T, Ohishi Y. All-fiber mode-locked laser based on Mamyshev mechanism with high-energy pulse generation at 1550 nm. *J Lightwave Technol*. 2020;38(6):1468–1473.
29. Ma C, Khanolkar A, Zang Y, Chong A. Ultrabroadband, few-cycle pulses directly from a Mamyshev fiber oscillator. *Photonics Res*. 2020;8(1):65–69.
30. Repgen P, Schuhbauer B, Hinkelmann M, Wandt D, Wienke A, Morgner U, Neumann J, Kracht D. Mode-locked pulses from a Thulium-doped fiber Mamyshev oscillator. *Opt Express*. 2020;28(9):13837–13844.
31. Xu S-S, Liu M, Wei Z-W, Luo AP, Xu WC, Luo ZC. Multipulse dynamics in a Mamyshev oscillator. *Opt Lett*. 2020;45(9):2620–2623.
32. Chen Y-H, Sidorenko P, Thorne R, Wise F. Starting dynamics of a linear-cavity femtosecond Mamyshev oscillator. *J Opt Soc Am B*. 2021;38(3):743–748.
33. Yan D, Li X, Zhang S, Liu J. Pulse dynamic patterns in a self-starting Mamyshev oscillator. *Opt Express*. 2021;29(7):9805–9815.
34. Poeydebat E, Scol F, Vanvincq O, Bouwmans G, Hugonnot E. All-fiber Mamyshev oscillator with high average power and harmonic mode-locking. *Opt Lett*. 2020;45(6):1395–1398.
35. Piechal B, Szczepanek J, Kardaś TM, Stepanenko Y. Mamyshev oscillator with a widely tunable repetition rate. *J Lightwave Technol*. 2021;39(2):574–581.
36. Wang T, Ren B, Li C, Wu J, Su R, Ma P, Luo ZC, Zhou P. Over 80 nJ sub-100 fs all-fiber Mamyshev oscillator. *IEEE J Sel Top Quantum Electron*. 2021;27(6):1–5.
37. Haig H, Sidorenko P, Thorne R, Wise F. Megawatt pulses from an all-fiber and self-starting femtosecond oscillator. *Opt Lett*. 2022;47(4):762–765.
38. Sun R, Jin D, Tan F, Wei S, Hong C, Xu J, Liu J, Wang P. High-power all-fiber femtosecond chirped pulse amplification based on dispersive wave and chirped-volume Bragg grating. *Opt Express*. 2016;24(20):22806–22812.
39. Mukhopadhyay PK, Ozgoren K, Budunoglu IL, Ilday FO. All-fiber low-noise high-power femtosecond Yb-fiber amplifier system seeded by an all-normal dispersion fiber oscillator. *IEEE J Sel Top Quantum Electron*. 2009;15(1):145–152.
40. Bednyakova A, Kuprikov E, Geraseva I, Kokhanovskiy A. Influence of spectral filtration on pulse dynamics in ring-cavity Mamyshev oscillator. *Appl Sci*. 2021;11(21):10398.
41. Perego AM. High-repetition-rate, multi-pulse all-normal-dispersion fiber laser. *Opt Lett*. 2017;42(18):3574–3577.
42. Liu X, Pang M. Revealing the buildup dynamics of harmonic mode-locking states in ultrafast lasers. *Laser Photonics Rev*. 2019;13(9):1800333.
43. Sidorenko P, Fu W, Wise F. Nonlinear ultrafast fiber amplifiers beyond the gain-narrowing limit. *Optica*. 2019;6(10):1328–1333.